

# Online Research @ Cardiff

This is an Open Access document downloaded from ORCA, Cardiff University's institutional repository: <https://orca.cardiff.ac.uk/id/eprint/97826/>

This is the author's version of a work that was submitted to / accepted for publication.

Citation for final published version:

Pullin, Rhys ORCID: <https://orcid.org/0000-0002-2853-6099>, Wright, Bryan J., Kapur, Richard, McCrory, John, Pearson, Matthew R. ORCID: <https://orcid.org/0000-0003-1625-3611>, Evans, Samuel Lewin ORCID: <https://orcid.org/0000-0003-3664-2569> and Crivelli, Davide ORCID: <https://orcid.org/0000-0002-1573-5726> 2017. Feasibility of detecting orthopaedic screw overtightening using acoustic emission. Proceedings of the Institution of Mechanical Engineers, Part H: Journal of Engineering in Medicine 231 (3) , pp. 213-221. 10.1177/0954411916689112 file

Publishers page: <http://dx.doi.org/10.1177/0954411916689112>  
<<http://dx.doi.org/10.1177/0954411916689112>>

Please note:

Changes made as a result of publishing processes such as copy-editing, formatting and page numbers may not be reflected in this version. For the definitive version of this publication, please refer to the published source. You are advised to consult the publisher's version if you wish to cite this paper.

This version is being made available in accordance with publisher policies.

See

<http://orca.cf.ac.uk/policies.html> for usage policies. Copyright and moral rights for publications made available in ORCA are retained by the copyright holders.



# Feasibility of detecting orthopedic screw overtightening using Acoustic Emission

Rhys Pullin<sup>1</sup>, Bryan J. Wright<sup>2</sup>, Richard Kapur<sup>1</sup>, John P. McCrory<sup>1</sup>, Matthew Pearson<sup>1</sup>, Sam L. Evans<sup>1</sup>, Davide Crivelli<sup>1\*</sup>

<sup>1</sup>Cardiff University, Cardiff School of Engineering, Queen's Building, The Parade, Cardiff CF24 3AA, Wales, United Kingdom

<sup>2</sup>Ringerike Sykehus, Orthopedic Department, Hønefoss, Norway

\* corresponding author

e-mail: [crivellid@cardiff.ac.uk](mailto:crivellid@cardiff.ac.uk), tel. +44(0)29 2087 5924

## Abstract

A preliminary study of Acoustic Emission during orthopaedic screw fixation was performed using polyurethane foam as the bone-simulating material. Three sets of screws, a Dynamic Hip Screw, a small fragment screw and a large fragment screw were investigated, monitoring acoustic emission activity during the screw tightening. Some specimens were overtightened on purpose to investigate the possibility of identifying the stripping torque before stripping actually occurred. One set of data was supported by load cell measurements to directly measure the axial load through the screw.

Data showed that Acoustic Emission can give good indications of impending screw stripping; such indications are not available to the surgeon at the current state of the art using traditional torque measuring devices, and current practice relies on the surgeon's experience alone. The results suggest that Acoustic Emission may have the potential to prevent screw overtightening and bone tissue damage, eliminating one of the commonest sources of human error in such scenarios.

**Keywords:** Acoustic Emission, Biomedical Devices, Medical Signal Processing, Orthopaedic Procedures, Orthopaedic Screws

# 1 Introduction

Bone fracture fixation is a common yet very complex task in orthopaedic surgery. When two ends of a fractured bone have to be held together an orthopaedic surgeon will use a number of methods to obtain stability at the fracture site. The two fracture ends must be restrained in a way in which relative movements are limited in order to promote healing and minimize deformations<sup>1,2</sup>.

One of the commonest procedures in orthopaedic surgery is the open reduction and internal fixation of an ankle fracture. Often screws are placed into the metaphyseal bone of the lateral malleolus in combination with a plate with metaphyseal screws alone used to secure the medial malleolus and maintain anatomical reduction.

During screw fixation the surgeon relies on experience to judge how much torque is required for the optimal hold in the bone. An accidental overtightening can cause stripping of the bone tissue around the screw. As shown by Tsuji et al<sup>3</sup>, the bone mechanical characteristics can vary widely among patients and bone tissues; moreover, orthopaedic surgeons currently rely on a “plateau” characteristic of the torque response<sup>4</sup> (i.e. the resisting torque stops increasing at a certain point) to decide when to stop turning. This stopping torque is very close to the stripping torque and so a very high degree of precision and experience is required, and often not sufficient, to avoid screw overtightening.

When a screw is overtightened the structural bonds of the surrounding cancellous bone can be broken and the load bearing capacity of the fixation can decrease dramatically. If the screw fails to hold the fracture fixation in a stable position, post-operative complications (such as increased fracture healing time, fibrous non-union of the fracture or a mal-position of the articular surface or the fracture) or premature failure of the implant may occur<sup>5-7</sup>.

Torque meters and torque limited screwdrivers have been proven to be ineffective in determining the stopping torque of a bone implant screw<sup>3</sup>. A sensor or set of sensors able to detect the onset of bone damage, instead of relying on torque, may help surgeons on deciding the stopping point during screw tightening.

When a material experiences irreversible damage energy is released in the form of heat and elastic waves. The latter, when observed in the ultrasonic frequency band, is referred to as Acoustic Emission (AE). Monitoring AE is a well-established Non Destructive Testing (NDT) technique - a non-invasive method of crack detection used in the engineering and Structural Health Monitoring (SHM) field<sup>8,9</sup> (Figure 1). Piezoelectric transducers, with a typical frequency response band lying between 10kHz to 1Mhz, when adhered to the surface of the structure to be tested can detect and record such ultrasonic waves. Data analysis techniques make it possible to assess and localise the failure or fracture of a material. It is established in the AE and NDT community that the rate of AE emission and the energy content of the signals are closely related to damage<sup>10</sup>.

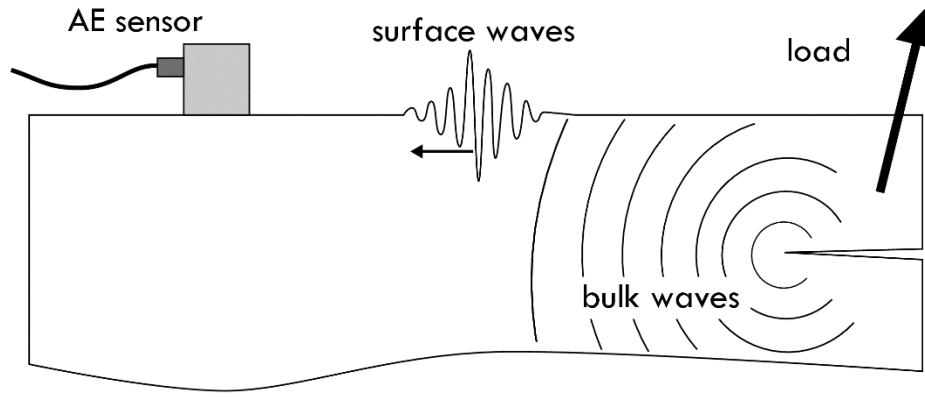


Figure 1: AE working principle

Shrivastava and Prakash<sup>11</sup> provided a review of the use of AE in the biomedical field, in particular regarding the application of the technique to orthopaedics. They highlight how AE activity can be an indicator of the ongoing fracture processes and demonstrate the negligible effect of the presence of soft tissue. Some authors highlighted such negligible effect<sup>12</sup>; others have found some correlation between the bone mechanical conditions and the AE signals<sup>13</sup>, also highlighting the presence of AE activity during human femur fracture processes<sup>14</sup>.

A real-time monitoring system, capable of detecting the proper tightening or the onset of overtightening of an implanted screw, may make it possible to improve the patient's healing and help reduce human error in bone surgery. The aim of this study was to demonstrate the feasibility of using AE in detecting the onset of screw stripping in a Dynamic Hip Screw (DHS), a partially threaded 3.5mm cancellous bone small fragment screw and a 4.5mm large fragment screw.

## 2 Material and Methods

Three different sets of tests were performed. The first two sets consist of 6 individual tests each, while the third set consists of 5 individual tests. A total of 17 datasets were collected. The first set concerned the possibility to detect AE signals through the screw by attaching the sensor directly to it ("Sensor on screw" tests). A second set of tests explored the possibility of recording AE signals by attaching the sensor directly to the screwdriver ("Sensor on screwdriver" tests). For each set of tests, 3 tests were conducted trying to overtighten the screws on purpose; the other 3 tests were conducted stopping the tightening process prior to damaging the bone, as would normally happen during a routine surgical screw fixation. The third test utilized a load cell to measure the axial load on a 55mm large fragment screw (4.5mm diameter). A summary of the different setups, along with specimen encoding, is shown in Table 1.

Table 1: Summary of the different test setups

Code	Samples	Stripped	Sensor placement	Screw type	Screwdriver type
SW_S	3	Yes	Screw	12.7mm DHS	Quick coupling T-handle with strain gauge
SW_N	3	No			
SD_S	3	Yes	Screwdriver	3.5mm partially threaded cancellous bone screw	Small fragment screwdriver (no strain gauge)
SD_N	3	No			
AX	5	Yes	Load cell	4.5mm large fragment screw	Large fragment screwdriver (no strain gauge)

Artificial bone testing blocks made of polyurethane foam<sup>a</sup> were used. The blocks had a size of 13cm×18cm×4cm. The density of the foam block was 240 kg/m<sup>3</sup>, which falls in the range of human cancellous bone density, 100 to 1000 kg/m<sup>3</sup><sup>15</sup>. These coupons are commonly used during training and are believed to satisfactorily represent the mechanical properties of the bone: as an example, they are employed in ASTM standard tests for medical screws pullout<sup>16</sup>.

Pre-drilling was performed for all test sets as is standard Orthopaedic practice. Tapping was performed prior to screw tightening for the SW and AX sets (dynamic hip and large fragment screws).

All test sets were conducted with a single AE sensor setup. The sensor used was a Pancom Pico Z, which has a frequency response band of 200-500 kHz. The AE sensor was connected to a measurement chain, consisting of a pre-amplifier and digital signal processing unit; signals, consisting of AE hits and their parameters, were recorded and stored by the unit. No additional filters were applied to signals. The AE system records every transient waveform that exceeds the 50dB<sub>AE</sub><sup>b</sup> pre-set threshold, and calculates a number of parameters. Of interest on this study is the event energy (sometimes referred to as Measured Area of the Rectified Signal Envelope, or MARSE), which is accepted in the AE research community to be closely related to damage<sup>10,17</sup>.

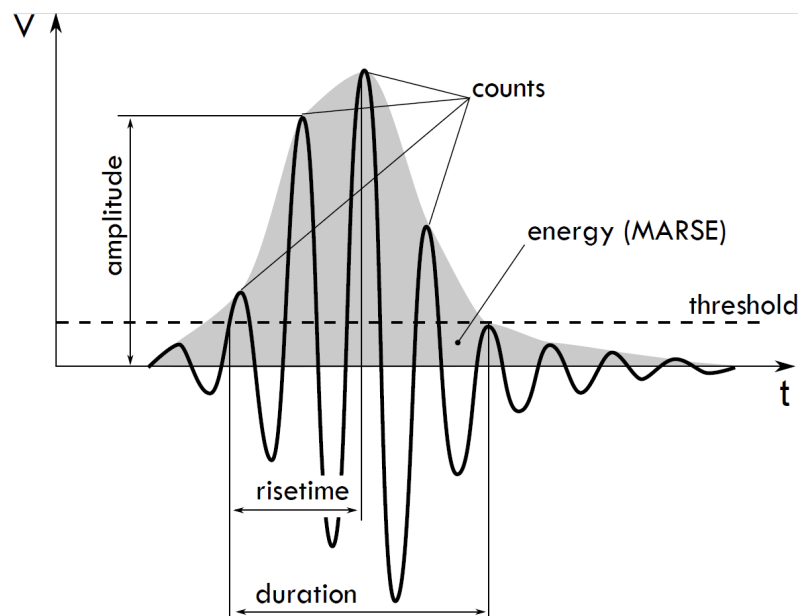


Figure 2: Acoustic Emission “hit” and its typical parameters

In addition to recording traditional AE parameters, an Artificial Neural Network (ANN) technique, described by Crivelli et al<sup>18</sup>, was used to identify natural groups (called “classes”) of AE signals with similar characteristics: it has been proven that the technique is able to discriminate and identify different damage modes in composite materials<sup>18–20</sup>. The technique is based on using a particular class of Artificial Neural Networks called Self-Organizing Map (SOM)<sup>21</sup> which is capable of classifying datasets based on their relative distance. Usually, the number of neurons in SOM is much higher than the expected signal clusters; to provide a coarser classification the SOM distance map is clustered with the k-means algorithm<sup>22</sup>. The optimal number of clusters is then chosen automatically based on a number of clustering quality indexes, based on the work of Sause et al<sup>23</sup>

<sup>a</sup> Sawbones (Vashon, WA, USA), model 1522-02

<sup>b</sup> dB<sub>AE</sub> are defined using a reference of 1 pV at the sensor



and further detailed in <sup>18</sup>. The parameters used in this study were Risettime, Counts, Absolute Energy, Duration, Amplitude, Average Frequency, Reverberation Frequency, Counts to Peak.

## 2.1 Sensor on screw

A standard DHS set<sup>c</sup> was used for these tests. The quick coupling T-handle included in the set was modified by attaching two shear strain gage rosettes to the handle body; the rosette signals were acquired by the AE system through the conditioning unit outputs<sup>d</sup>, which allowed synchronisation of the AE activity with the torque acting on the screwdriver. After pre-drilling the AE sensor was mounted to the screw with cyanoacrylate glue. The sensitivity and the correct bonding of the AE sensor were then verified using a standard pencil lead breaking test<sup>24</sup>. The 12.7mm DHS screw was then screwed in until stripping for the 3 SW\_S tests; the other 3 SW\_N tests were performed with a tight fit which, according to the experienced operator, coincided with the recording of a high amplitude AE event (higher than 80dB<sub>AE</sub>).

## 2.2 Sensor on screwdriver

A standard small fragment partially threaded 3.5mm cancellous bone screw<sup>c</sup> was screwed into the pre-drilled 2.5mm hole in the testing block. Between the screw and the testing block, a Dynamic Compression Plate (DCP) from the screw kit was fitted together with another metal plate, which was used for stabilizing the construct in the vice and to enable an even pull out test. The AE sensor was bonded with cyanoacrylate glue to the screwdriver shaft. The test set-up is shown in Figure 3.

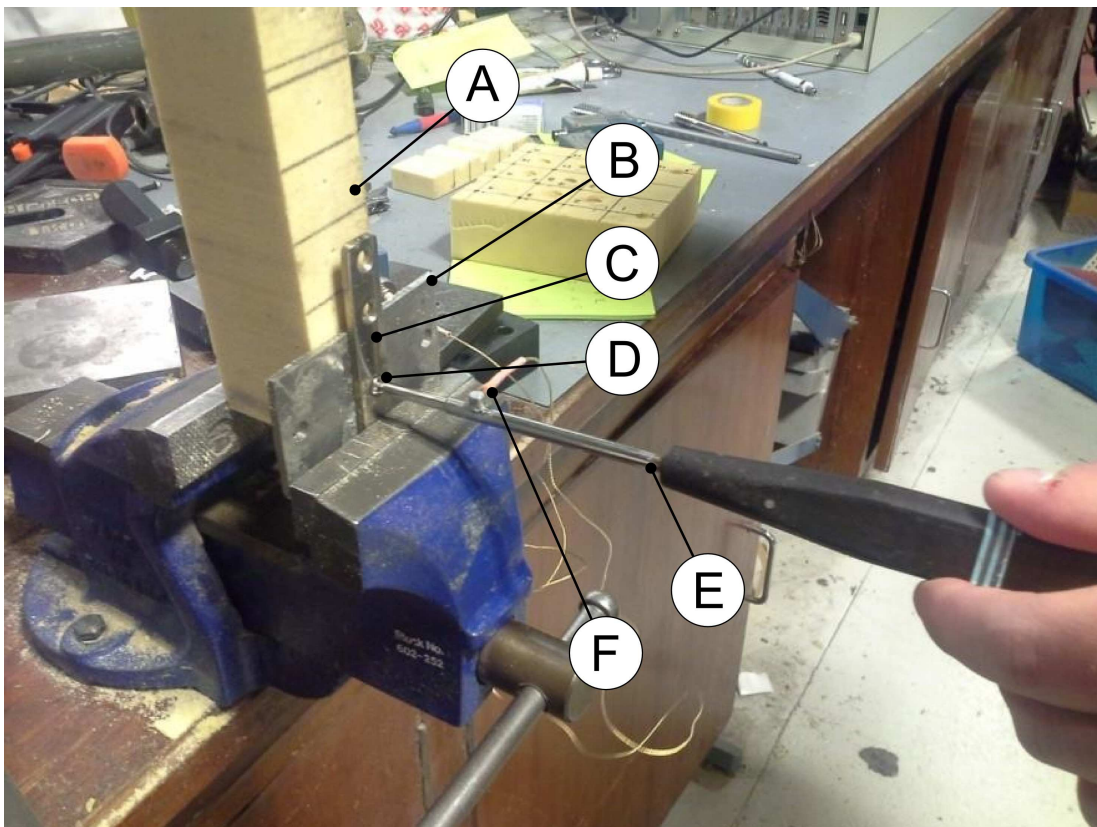


Figure 3: Sensor on screwdriver setup during screw fixation: testing block (A), metal plate (B) for pull out, DCP plate (C) and screw (D). small fragment screwdriver (E) is shown with the bonded AE sensor (F).

<sup>c</sup> Depuy Synthes Johnson & Johnson Medical, Capitol Boulevard, Capital Park, Leeds, UK

<sup>d</sup> P3 Strain Indicator and Recorder, Vishay Precision Group, Raleigh, NC USA

### 2.3 Pull tests procedure

To evaluate the different load bearing capacity of a stripped and a non-stripped screw assembly pull tests were performed on a 50kN uniaxial hydraulic testing machine<sup>e</sup>. The axial force and displacement were recorded throughout the test. The setup is shown in Figure 4

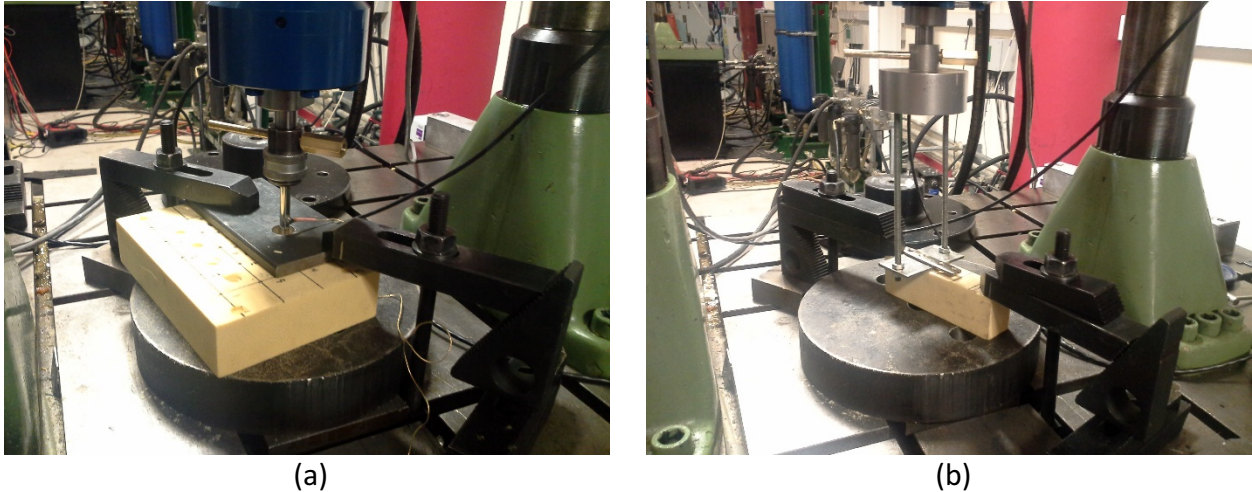


Figure 4: DHS (a) and small fragment screw (b) pullout setups

### 2.4 Axial load cell

To address on-going inaccuracy of measuring the point of thread stripping the new approach incorporated a strain gauge load cell. This was a half bridge system using the same hardware setup as described above. The height of the load cell (28mm) meant a longer screw was required to span it therefore switching to a large fragment screw (55mm in length, 4.5mm diameter) was necessary. The third experimental setup model is shown in Figure 5. Preliminary testing demonstrated successful recording of the tensile strain and clearly demonstrated a drop on thread stripping. Five definitive datasets were collected using this setup. AE waveform data was also recorded during the experiments.

---

<sup>e</sup> Losenhausen, Dusseldorf, Germany; control software: MTS Flextest GT Master, Eden Prairie, MN, USA

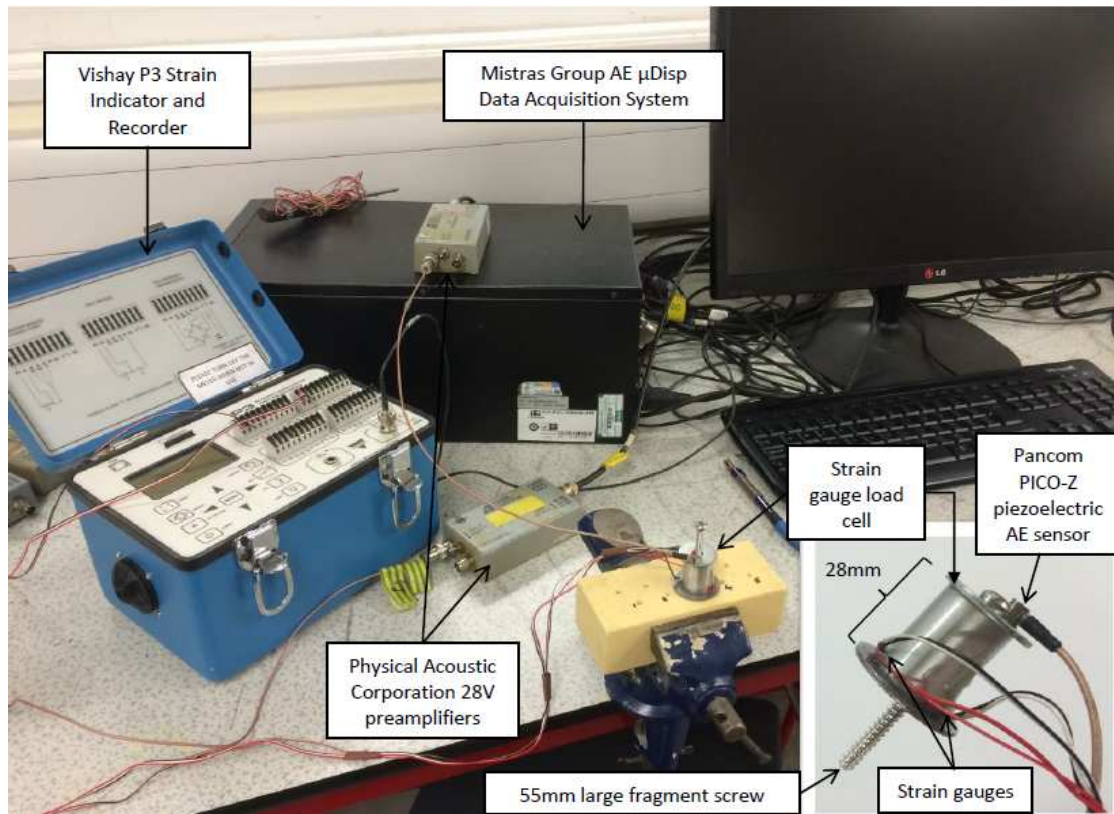


Figure 5: axial load cell test setup

### 3 Results

#### 3.1 AE during screw tightening

##### 3.1.1 Sensor on screw / DHS screws

Figure 6 shows AE cumulative energy (the sum of the energy of all AE events recorded) versus time, together with data from the strain gauge, for SW\_S\_01 (a stripped DHS screw).

Figure 7 shows AE energy data for stripped and non-stripped screws. The total AE energy output is not clearly linkable to stripping: traditional AE shows no evidence of any difference between the two groups. A more advanced and detailed data analysis was thus required.



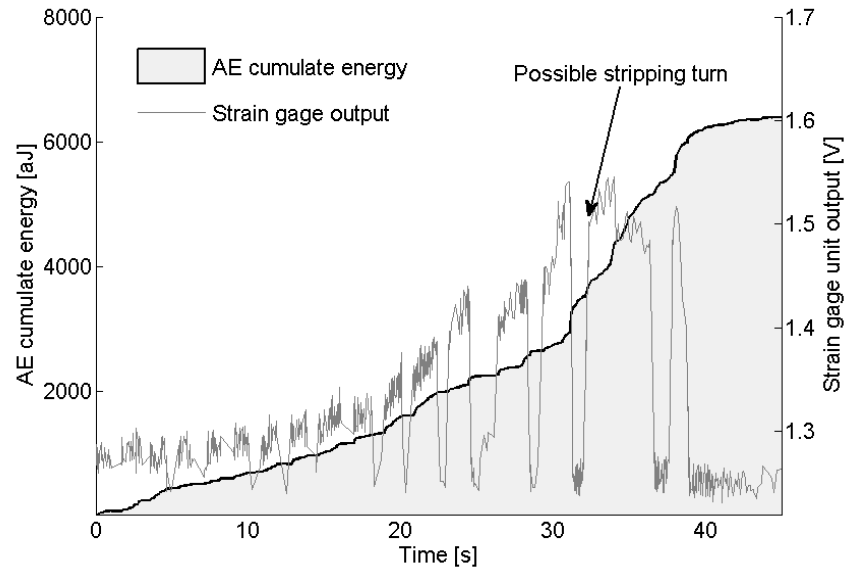


Figure 6: AE and strain gage output for SW\_S\_01

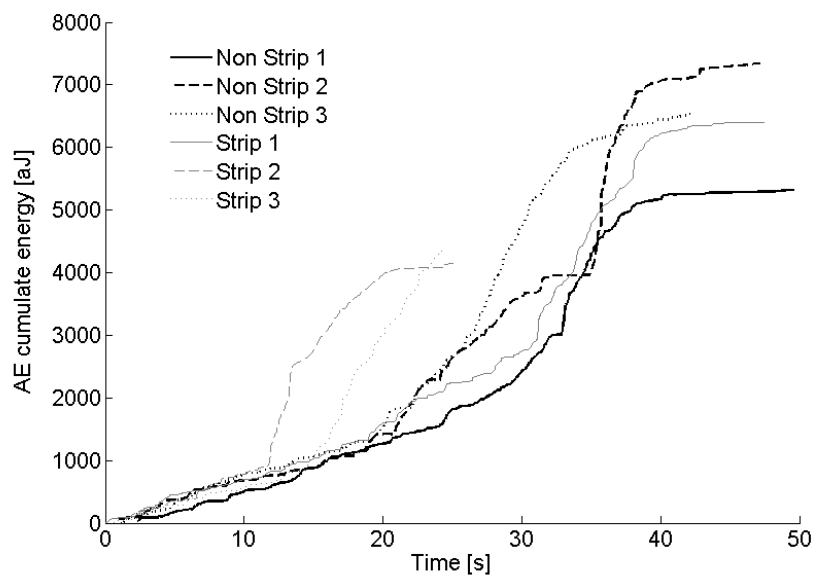


Figure 7: DHS screw energy comparison

### 3.1.2 Sensor on screwdriver

Figure 8 shows AE cumulative energy and AE events amplitude for small fragment screws. In this setup (AE sensor bonded on screwdriver) the energy levels are an order of magnitude higher, and one can identify and separate more clearly the stripped and the non-stripped screws: a knee with a consequential significantly increasing trend in the AE cumulative energy in a short timespan is clearly identifiable.

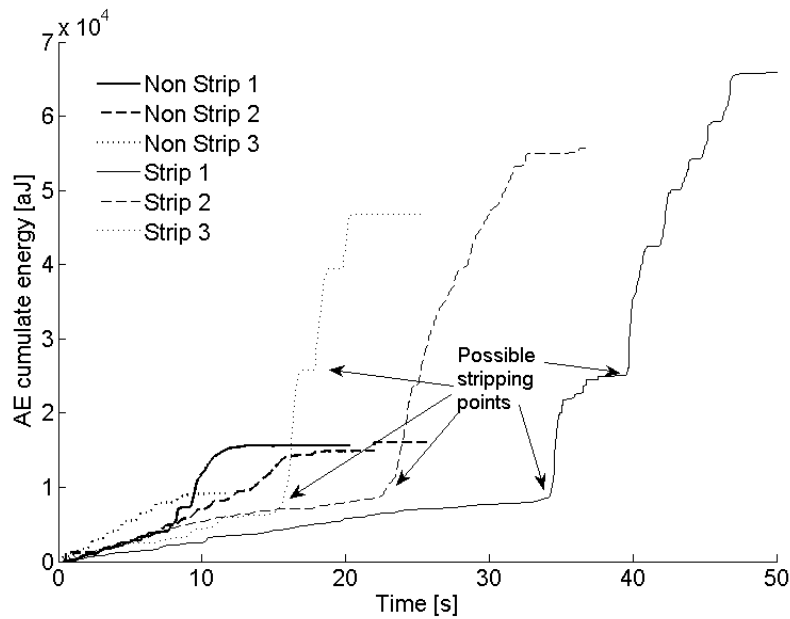


Figure 8: Small fragment screw AE data

### 3.2 Pull tests

During pull-tests the load-displacement characteristics of both sets showed significant differences among stripped and non-stripped screws. The curves can be seen in Figure 9a (DHS) and Figure 9b (small fragment screw assemblies).

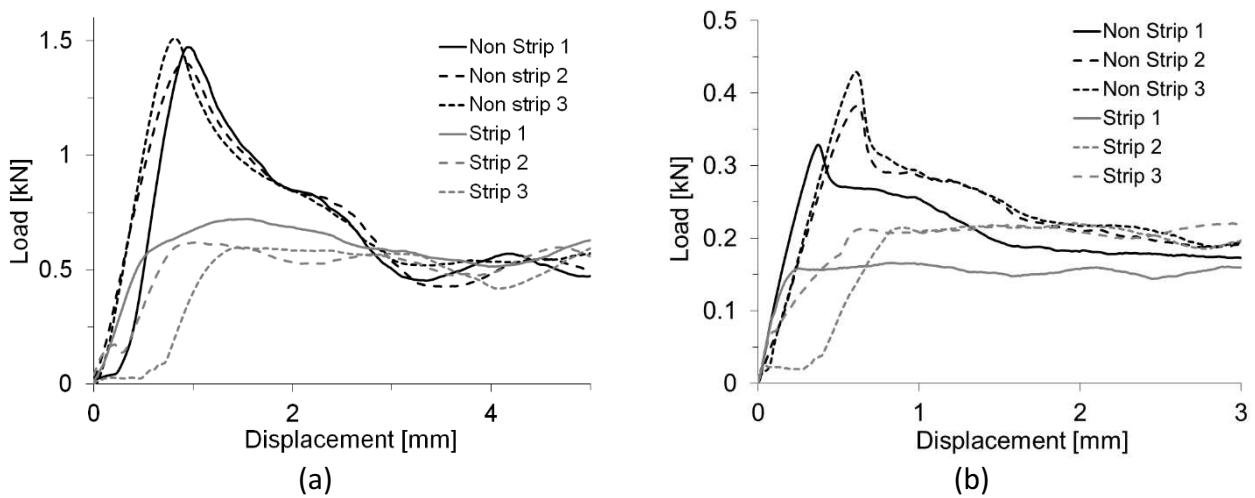


Figure 9: pull-out curves of DHS (a) and small fragment (b) screw assemblies

### 3.3 Specimens failure analysis and observations

Figure 10 shows a cut-out cross section of a non-stripped thread and a stripped thread. The conditions of the stripped thread clearly shows that the threads in the bone-like material were damaged in a way that did not guarantee a proper load transmission. This easily explains the different tensile behaviour of stripped and non-stripped screws.

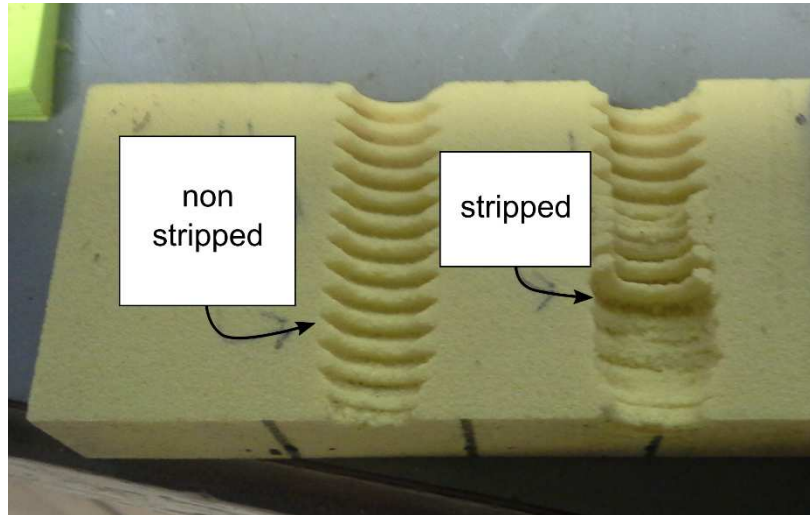


Figure 10: examination of a non-stripped and a stripped thread after screw fixation

### **3.4 Augmented AE with ANN**

Due to the inherent difficulties in interpreting data for the DHS setup the above mentioned ANN classification technique was applied to the dataset. The classification procedure lead to the identification of two classes. Figure 11 shows the trend of the two AE classes for 4 different specimens; cumulative energy is in this case reset after each screwdriver turn. Figure 11 a and b show tests from non-stripped samples; Figure 11 c and d show tests from stripped samples. The number of AE hits in each screwdriver turn is also shown.

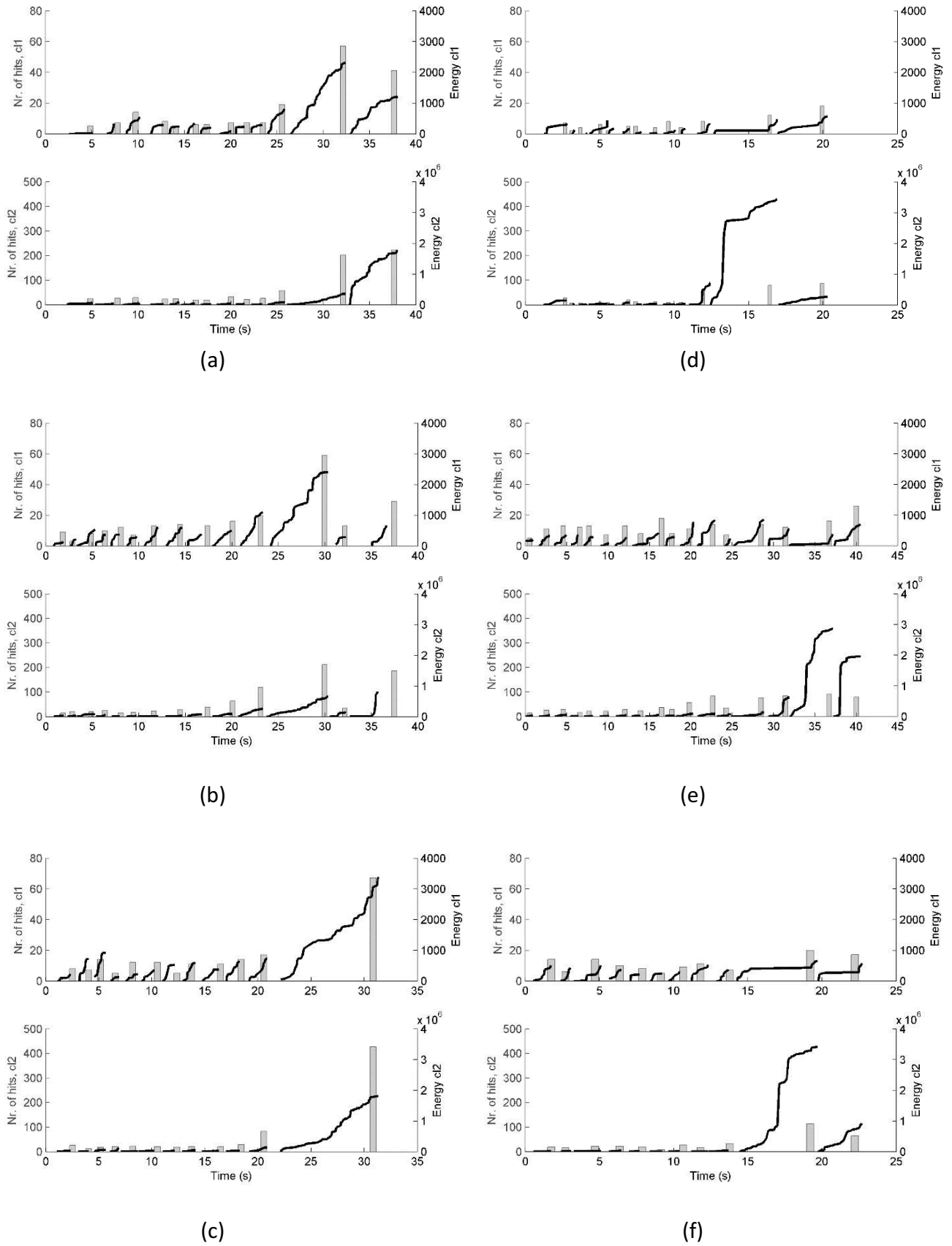


Figure 11: DHS tests after AE classification: non-stripped (a, b, c) and stripped (d, e, f) screw tests.



### 3.5 Determination of stopping criteria on axially loaded screw

The same ANN analysis procedure was applied to the sensor on load cell set. Strain was normalized to the maximum axial strain measured by the load cell, meaning maximum axial load on the screw and therefore optimal screw fixation. Figure 12 shows the results for Class 1 (a) and Class 2 (b) energy. By examining Class 2 energy an optimal point of screw tightening can be observed. The figures show the fixation process as AE energy accumulates: at first, strain is low and increasing and AE is accumulating. At a certain AE energy level strain stops increasing (i.e. the screw thread / implant interface begins to crush). From that point on AE energy continues to accumulate as damage progresses and strain decreases as the screw assembly progressively loses its capability to transfer axial force due to damage in the sawbone material.

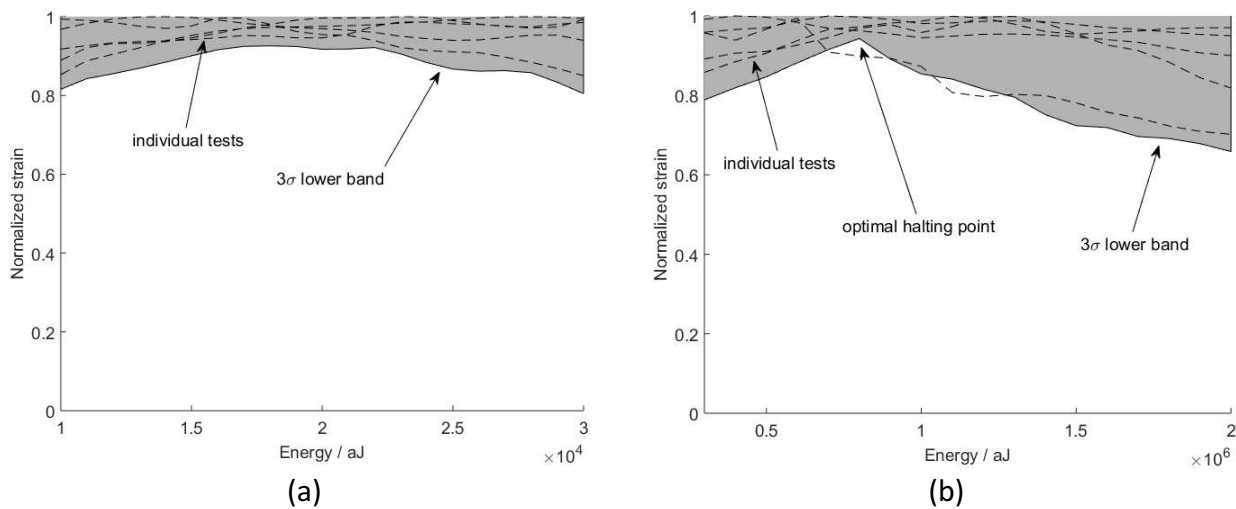


Figure 12: AE/ANN axial loadcell setup: class 1 (a) and class 2 (b).

## 4 Discussion

Visible differences were highlighted among stripped and non-stripped test blocks in terms of pullout strength (Figure 9). In particular, the correctly fixed screws showed in both sets a quasi linear-elastic force-displacement characteristic, with a distinctive peak and a decrease at higher displacement values. The stripped screw assemblies showed no peak behaviour; instead they reached a plateau at around the same displacement as the correctly fixed screws; the plateau value is similar to the high-displacement axial force in non-stripped tests. This may be explained by considering the low displacement region dominated by homogeneous load transfer between the screw threads (if correctly fixed) and the bone-like material; then, the contact region at the screw location becomes damaged and the load transfer proceeds by means of shear or crushing.

The load bearing capacity of stripped screw assemblies was approximately 50%-60% lower than the correct assembly. This, in a real-life bone and screw assembly (typically load-controlled and not displacement controlled), confirms that the load bearing and energy absorption capacity of such an implant highly depends on a correct screw fixation<sup>4,25</sup>.

AE events were recorded in both set-ups. A correlation between AE energy and damage occurring in the material can be inferred from the high rate of energy that can be seen close to the stopping / stripping torque. AE energy alone was however not sufficient to provide any information in the

DHS setup. In the sensor on screwdriver setup stripped screws showed an overall higher energy level, one or two orders of magnitude higher than in non-stripped screws.

The classification of AE signals during the sensor on screw tests also made it possible to obtain a better insight into the damage mechanisms that occur during screw fixation (Figure 11). Class 1 events have an almost constant rate of energy release and show comparable energy levels per turn. The smooth increase in energy suggests that these events are related to screw thread friction or to the screw thread cutting/shearing the material. Class 2 events show instead high energy jumps, related to short-time energy release mechanisms. Moreover, high energy release in class 2 happens in more than one turn in overtightened screws compared to barely at the end of a single turn in correctly fitted screws. This suggests that class 2 AE events may be linked to crushing damage. In correctly fitted screws a small amount of damage is required to obtain a sufficient screw axial preload. When this damage becomes too high the material around the screw thread loses part of its load bearing capacity. This results in the screw not providing the axial force required to transfer the load via friction to the implant plates, resulting in the load – displacement curve plateauing as seen in the pullout tests.

By measuring the axial load during screw insertion it has been shown that a threshold in AE energy can be set in order to determine the stopping criterion. In a real implant there will be no access to axial force measurement however the two initial tests have shown that AE can be measured through the screwdriver. The third experiment shows that thresholding is, indeed, feasible for providing an early indication of screw stripping.

As previously discussed, torque meters and torque limited screwdrivers have been proven to be ineffective in determining the stopping torque of a bone implant screw<sup>3</sup>. By demonstrating the feasibility of early detection of screw overtightening using AE based on the bone AE energy, a surgical screwdriver can be manufactured in such a way that it could incorporate, or allow the fixing of, a small footprint AE sensor. The instrument may provide alarms to the surgeon based on predetermined thresholds in a way that no expertise in the use of AE is required. The only major hurdle in implementing such a device at the moment is the lack of live bone AE measurements. As the presence of soft tissue has already been proven not to significantly affect AE signals<sup>12</sup>, once the screwdriver design is determined this may be overcome easily by designing an experimental plan which takes into account different bone and implant types.

## 5 Conclusions

An experimental campaign to test AE monitoring of screw fixation in bone-like testing blocks was performed using three different types of screw assemblies and test scenarios. AE activity was recorded; AE amplitude was used as a stopping criterion for determining correct screw tightening. A deeper analysis of AE data with an unsupervised neural network-based classification technique showed two different damage mechanisms that could be helpful to detect overtightened screws.

Surgeons make decisions on when to stop tightening a screw based on experience and tactile feedback. This can easily lead to incorrect fixation, especially in the initial phases of surgical experience, during training or when dealing with an unexpected bone mechanical condition. The use of torque limiting screwdrivers has proven to lack the accuracy and the sensitivity required to deal with different bone densities. The preliminary study presented in this paper shows that a device which employs AE monitoring to detect the stopping condition could be of significant benefit to Orthopaedic surgeons during bone fixation, and indeed during training.

As feasibility has been demonstrated a follow-up study with more characteristic conditions, e.g. adopting real bone models with different densities and surrounding tissue, will provide the further steps for validating this technique. The main points to address are the influence of in-vivo conditions on the detected AE signatures. The effect of surrounding tissues, different bone densities and conditions, and different screw thread types will all influence the AE transfer function therefore affecting the received signals. Moreover, the design of the device will have to take into account sterilizability and ergonomics as it will contain on-board electronics.

Due to the variations associated with patients and constructs, signals are likely to present differences; it is envisaged that the classification techniques presented in this paper will overcome this problem. However, to prove the robustness and statistical significance of the technique, a significant sample of in-vivo tests has to be conducted.

Once demonstrated in-vivo, the availability of such a device to surgeons could improve many aspects of Orthopaedics. First of all, during an operation the surgeon would have additional guidance as to when they are reaching the appropriate torque rather than relying on just their experience, as is currently the case. Secondly, this device could help surgeons to develop a higher sensitivity in the first phases of their hands-on training. As previously pointed out, optimal implant fixation reduces post-operative complications in patients and can guard against possible long-term sequelae, such as increased joint wear and post-operative arthritis. This would improve the quality of life for those patients and could significantly reduce the associated long-term healthcare costs to society.

## 6 References

1. Johnson KD, Tencer AF. *Biomechanics in Orthopedic Trauma*. 1st ed. CRC Press, [http://journals.lww.com/jorthotrauma/Abstract/1994/08060/Biomechanics\\_in\\_Orthopedic\\_Trauma.15.aspx](http://journals.lww.com/jorthotrauma/Abstract/1994/08060/Biomechanics_in_Orthopedic_Trauma.15.aspx) (1994, accessed 27 December 2014).
2. Lloyd J, Elsayed S, Hariharan K, et al. Revisiting the concept of talar shift in ankle fractures. *Foot Ankle Int*; 27: 793–796, <http://fai.sagepub.com/content/27/10/793.short> (2006, accessed 27 December 2014).
3. Tsuji M, Crookshank M, Olsen M, et al. The biomechanical effect of artificial and human bone density on stopping and stripping torque during screw insertion. *J Mech Behav Biomed Mater*; 22: 146–156, <http://www.sciencedirect.com/science/article/pii/S1751616113000866> (2013, accessed 27 November 2014).
4. Reynolds KJ, Cleek TM, Mohtar AA, et al. Predicting cancellous bone failure during screw insertion. *J Biomech*; 46: 1207–10, <http://www.ncbi.nlm.nih.gov/pubmed/23466167> (2013, accessed 27 November 2014).
5. Flores LA, Harrington IJ, Heller M. The stability of intertrochanteric fractures treated with a sliding screw-plate. *J Bone Joint Surg Br* 1990; 72: 37–40.
6. Thomas AP. Dynamic hip screws that fail. *Injury* 1991; 22: 45–46.
7. Kim WY, Han CH, Park JI, et al. Failure of intertrochanteric fracture fixation with a dynamic hip screw in relation to pre-operative fracture stability and osteoporosis. *Int Orthop* 2001; 25: 360–362.

8. Pao Y. Theory of Acoustic Emission. *Elastic Waves NDT Mater* 1978; 29: 107–127.
9. Finlayson RD. Acoustic Emission Testing. In: Hellier C (ed) *Handbook of Nondestructive Evaluation*. New York: McGraw-Hill, 2003, pp. 10.1 – 10.39.
10. Bourchak M, Farrow I, Bond I, et al. Acoustic emission energy as a fatigue damage parameter for CFRP composites. *Int J Fatigue*; 29: 457–470, <http://linkinghub.elsevier.com/retrieve/pii/S0142112306001721> (2007, accessed 19 July 2011).
11. Shrivastava S, Prakash R. Assessment of bone condition by acoustic emission technique: A review. *J Biomed Sci Eng*; 02: 144–154, <http://file.scirp.org/Html/432.html> (2009, accessed 27 December 2014).
12. Wright TM, Carr JM. Soft Tissue Attenuation of Acoustic Emission Pulses. *J Biomech Eng*; 105: 20, <http://biomechanical.asmedigitalcollection.asme.org/article.aspx?articleid=1396071> (1983, accessed 27 December 2014).
13. Leichter I, Bivas A, Margulies JY, et al. Acoustic emission from trabecular bone during mechanical testing: the effect of osteoporosis and osteoarthritis. In: *Proceedings of the Institution of Mechanical Engineers, Part H: Journal of Engineering in Medicine* 1989-1996 (vols 203-210), pp. 123–127, [http://pih.sagepub.com/lookup/doi/10.1243/PIME\\_PROC\\_1990\\_204\\_241\\_02](http://pih.sagepub.com/lookup/doi/10.1243/PIME_PROC_1990_204_241_02) (1990, accessed 27 December 2014).
14. Strantza M, Louis O, Boulpaep F, et al. Acoustic Emission on Human Femur Tissue Fracture. In: *31st Conference of the European Working Group on Acoustic Emission (EWGAE)*, pp. 1–8, <http://file.scirp.org/Html/432.html> (2014).
15. ASTM F1839-08(2012), Standard Specification for Rigid Polyurethane Foam for Use as a Standard Material for Testing Orthopaedic Devices and Instruments, [www.astm.org](http://www.astm.org) (2012, accessed 12 January 2015).
16. ASTM F543-07. Standard Specification and Test Methods for Metallic Medical Bone Screws, <http://scholar.google.com/scholar?hl=en&btnG=Search&q=intitle:Standard+Specification+and+Test+Methods+for+Metallic+Medical+Bone+Screws#0> (2012).
17. Miller RK, McIntire P. NDT Handbook vol. 5. American Society for Nondestructive Testing, 1987, p. 652.
18. Crivelli D, Guagliano M, Monici A. Development of an artificial neural network processing technique for the analysis of damage evolution in pultruded composites with acoustic emission. *Compos Part B Eng*; 56: 948–959, <http://www.sciencedirect.com/science/article/pii/S1359836813005180> (2014, accessed 16 December 2014).
19. Crivelli D, Guagliano M, Eaton M, et al. Localisation and identification of fatigue matrix cracking and delamination in a carbon fibre panel by acoustic emission. *Compos Part B Eng*; 74: 1–12, <http://www.sciencedirect.com/science/article/pii/S1359836815000049> (2015).
20. McCrory JP, Al-Jumaili SK, Crivelli D, et al. Damage classification in carbon fibre composites using acoustic emission: A comparison of three techniques. *Compos Part B Eng*; 68: 424–430,



<http://www.sciencedirect.com/science/article/pii/S1359836814003849> (2015, accessed 11 December 2014).

21. Kohonen T. The self-organizing map. *Proc IEEE* 1990; 78: 1464–1480.
22. N Godin S Huguet RG. Integration of the Kohonen's self-organizing map and k-means algorithm for the segmentation of the AE data collected during tensile tests on cross-ply composites. *NDT E Int* 2005; 38: 299–309.
23. Sause MGR, Gribov A, Unwin AR, et al. Pattern recognition approach to identify natural clusters of acoustic emission signals. *Pattern Recognit Lett* 2012; 33: 17–23.
24. Hsu N. A Mechanical AE Simulator for System Calibration and Waveform Analysis. *16th Meet US Acoust Emiss Work Gr*, <http://scholar.google.com/scholar?hl=en&btnG=Search&q=intitle:A+mechanical+AE+simulator+for+system+calibration+and+waveform+analysis#0> (1976, accessed 19 December 2014).
25. Chapman JR, Harrington RM, Lee KM, et al. Factors affecting the pullout strength of cancellous bone screws. *J Biomech Eng* 1996; 118: 391–398.